408 *KSME International Journal, Vol. 11, No. 4, pp. 408~418, 1997*

Analysis for a Planar 3 Degree-of-Freedom Parallel Mechanism with Actively Adjustable Stiffness Characteristics

Whee-Kuk Kim*, Jun-Yong Lee* and Byung Ju Yi**

(*Received September 4, 1996*)

A planar three degree-of-freedom parallel manipulator has been extensively studied as the fundamental example of general parallel manipulators. It is proven from previous work (Kim, et. al., 1996) that when three identical joint compliances are attached to the three base joints of the mechanism in its symmetric configurations, this mechanism possesses a completely decoupled compliance characteristic at the object space, which is the important operational requirement for an RCC device. In this work, we are concerned with the adjustability of the output compliance matrix of this mechanism, by employing redundancy on either joint compliances or on actuators. Two approaches are suggested to achieve this purpose. In the first approach, the stiffness modulation is achieved through purely redundant passive springs or decoupled feedback stiffness gains. In the second approach, stiffness modulation is achieved through antagonistic actuation of the system actuators. General stiffness models are derived for both cases. Based on these stiffness models, stiffness modulation algorithms are formulated. The capability of actively adjustable stiffness will be very effective in several robotic applications.

Key Words: Remote Center Compliance(RCC), Planar Parallel Mechanism, Antagonistic Stiffness, Compliance Modulation, Adjustable Stiffness.

1. Introduction

Tasks such as electronic part assembly requiring high precision cannot be successfully performed by position-controlled robot manipulators due to their limited precision. Other factors that hinder successful assembly operations include imprecise position and/or orientation of the assembly bed, position sensor errors of automated assembly systems, non-uniformity of assembly parts, and non-rigidity of real bodies. Consequently, jamming or wedging occurs quite often during assembly operation, which increases task completion time.

To cope with these problems, various control schemes have been proposed: force feedback control via force/torque sensor (McCallion, et. al., 1980), compliance model based control (Cutkosky, et. al., 1989; Peshkin, 1990), and compliance control using compliance devices such as Remote Center of Compliance (RCC) devices (Whitney, 1986; Brussel, et. al., 1986), compliant work stations, or using compliance effects such as air or gas stream, and magnetic force. In general, using passive compliance devices is cost-effective and increases the bandwidth and stability of the system, compared to control methods using force-feedback. Particularly, RCC devices among various compliance devices have been popularly employed in various assembly tasks in automation industry.

However, since most currently existing RCC devices have a fixed structure, they cannot adjust their compliance characteristics according to continuously changing operational conditions. Therefore, RCC devices with actively adjustable compliance characteristics are discussed in this work.

* Dept. of Control & Instrumentation Eng., Korea Univ.

** Dept. of Control & Instrumentation Eng., Hanyang Univ.

Recently, parallel mechanisms have been proposed as a candidate RCC device. Two parallel mechanisms (i. e., 3 DOF planar and spherical mechanism) have been proposed for this purpose. It has been shown that each of these mechanisms has an RCC point in its symmetric configurations (Kim, et. al., 1996a and 1996b). In order for these mechanisms to have the desired operational compliance characteristics at the RCC point, joint compliances can be adjusted either by properly replacing joint compliances with those having different magnitude, or by actively controlling compliance at joints utilizing pneumatic cylinders, for example. These functions are advantages of parallel devices over current RCC devices. Further, we claim that when redundant joint compliances are attached to those parallel mechanisms symmetrically, the adjustability of their RCC characteristics is improved. Two approaches are proposed. In the first approach, adaptable RCC characteristics are achieved purely by employing redundant passive or feedback compliance. In the second approach, it is achieved by antagonistic redundant actuation among system actuators.

This paper is organized as follows. Initially, in Sec. 2, first- and second-order kinematic analysis for the proposed planar and spherical mechanisms are described. Then, using these kinematic models, the output compliance matrices due to redundant joint compliances are obtained for these mechanisms. In Sec. 3, we derive a compliance model created by the internal forces due to redundant actuation among the system actuators. Based on the compliance model, a load distribution method is proposed to create the desired RCC characteristics. Simulations for both cases are carried out to corroborate the proposed theory. Lastly, we draw conclusions.

2. Modulation of Output Compliance Matrix Using Redundant Joint Compliances

2.1. Kinematics of a planar 3 DOF parallel mechanism (Kang, et. al., 1990)

The mechanism proposed in this paper consists

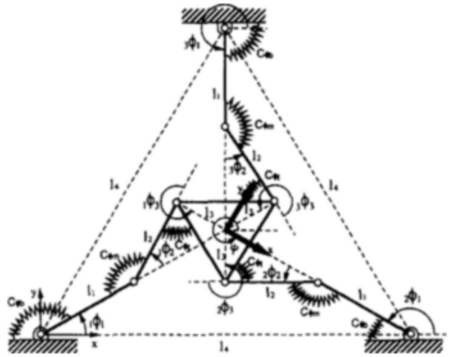

Fig. 1 A Planar 3 Degrees of Freedom Mechanism

of three subchains which connect the platform to the ground as shown in Fig. 1. Each subchain possesses three joints and two links. ${}_r\phi_n$ denotes the joint angle of the nth joint of the rth subchain. Also, ${}_rl_n$ denotes the link length of the nth link of the rth subchain. Let $\boldsymbol{u}=(x\ y\ \phi)^T$ represent the center location of the upper platform, and let ${}_r\boldsymbol{\phi}=({}_r\phi_1\ {}_r\phi_2\ {}_r\phi_3)^T$ represent the joint angles of the rth serial subchain. Then, the first- and second-order kinematic relations between the two vectors are described by (Freeman, et. al., 1988)

$$\dot{\boldsymbol{u}}=[{}_rG_\phi^u]{}_r\dot{\boldsymbol{\phi}},\quad r=1,2,3 \tag{1}$$

$$\ddot{\boldsymbol{u}}=[{}_rG_\phi^u]{}_r\ddot{\boldsymbol{\phi}}+{}_r\dot{\boldsymbol{\phi}}^T[{}_rH_{\phi\phi}^u]{}_r\dot{\boldsymbol{\phi}} \tag{2}$$

where $[{}_rG_\phi^u]$ and $[{}_rH_{\phi\phi}^u]$ represent the first- and second-order kinematic influence coefficient matrices, respectively. Assuming that $[{}_rG_\phi^u]$ is not singular, the inverse relation of the matrix is given by

$${}_r\dot{\boldsymbol{\phi}}=[{}_rG_\phi^u]^{-1}\dot{\boldsymbol{u}} \tag{3}$$

Here, we define $\boldsymbol{\phi}_b$, $\boldsymbol{\phi}_m$, $\boldsymbol{\phi}_t$ as the vectors which respectively consist of the three base joints, three second joints, and three third joints of the three-chain system. Each vector is given by

$$\boldsymbol{\phi}_b=({}_1\phi_1\ {}_2\phi_1\ {}_3\phi_1)^T \tag{4}$$

$$\boldsymbol{\phi}_m=({}_1\phi_2\ {}_2\phi_2\ {}_3\phi_2)^T \tag{5}$$

and

$$\boldsymbol{\phi}_t=({}_1\phi_3\ {}_2\phi_3\ {}_3\phi_3)^T \tag{6}$$

If we consider $\boldsymbol{\phi}_b$ as the active input, the first-order kinematic relation between the input vector and output vector can be obtained as

$$\dot{\boldsymbol{\phi}}_b=[G_u^b]\dot{\boldsymbol{u}} \tag{7}$$

where

$$[G_u^b]=\begin{bmatrix}[{}_1G_\phi^u]_{1;}^{-1}\\ [{}_2G_\phi^u]_{1;}^{-1}\\ [{}_3G_\phi^u]_{1;}^{-1}\end{bmatrix} \tag{8}$$

Here $[{}_iG_\phi^u]_{1;}^{-1}$ denotes the first row of $[{}_iG_\phi^u]^{-1}$. Assuming that $[G_u^b]$ is non singular, the inverse relation of Eq. (7) is

$$\dot{\boldsymbol{u}}=[G_b^u]\dot{\boldsymbol{\phi}}_b \tag{9}$$

where

$$[G_b^u]=[G_u^b]^{-1} \tag{10}$$

Likewise, the first-order kinematic relations for $\boldsymbol{\phi}_m$ and $\boldsymbol{\phi}_t$ are obtained respectively as

$$\dot{\boldsymbol{\phi}}_m=[G_u^m]\dot{\boldsymbol{u}} \tag{11}$$

$$\dot{\boldsymbol{\phi}}_t=[G_u^t]\dot{\boldsymbol{u}} \tag{12}$$

where

$$[G_u^m]=\begin{bmatrix}[{}_1G_\phi^u]_{2;}^{-1}\\ [{}_2G_\phi^u]_{2;}^{-1}\\ [{}_3G_\phi^u]_{2;}^{-1}\end{bmatrix} \tag{13}$$

$$[G_u^t]=\begin{bmatrix}[{}_1G_\phi^u]_{3;}^{-1}\\ [{}_2G_\phi^u]_{3;}^{-1}\\ [{}_3G_\phi^u]_{3;}^{-1}\end{bmatrix} \tag{14}$$

The proposed mechanism possesses nine joints. The minimum number of actuating joints is decided according to the system mobility. Since the mobility of the system is 3, at least, three joints should be activated to operate the mechanism. Let $\boldsymbol{\phi}_b$ be the independent joint vector ($\boldsymbol{\phi}_a$), and let the remaining joints $(\boldsymbol{\phi}_m{}^T, \boldsymbol{\phi}_t{}^T)^T$ be denoted by the dependent joint vector ($\boldsymbol{\phi}_p$). Then, the following relations are derived from Eqs. (7), (11), and (12):

$$\dot{\boldsymbol{\phi}}_m=[G_u^m][G_b^u]\dot{\boldsymbol{\phi}}_b=[G_b^m]\dot{\boldsymbol{\phi}}_b \tag{15}$$

$$\dot{\boldsymbol{\phi}}_t=[G_u^t][G_b^u]\dot{\boldsymbol{\phi}}_b=[G_b^t]\dot{\boldsymbol{\phi}}_b \tag{16}$$

Now, the first-order kinematic relation between the dependent joint vector and the independent joint vector is obtained by combining Eqs. (15) and (16), as below:

$$\dot{\boldsymbol{\phi}}_p=[G_b^p]\dot{\boldsymbol{\phi}}_b \tag{17}$$

where

$$[G_b^p]=\begin{bmatrix}[G_b^m]\\ [G_b^t]\end{bmatrix} \tag{18}$$

Meanwhile, the inverse relation of Eq. (2) is described by

$$_r\ddot{\boldsymbol{\phi}}=[{}_rG_\phi^u]^{-1}\ddot{\boldsymbol{u}}+\dot{\boldsymbol{u}}^T[{}^rH_{uu}^\phi]\dot{\boldsymbol{u}} \tag{19}$$

where

$$[{}^rH_{uu}^\phi]=-[{}_rG_\phi^u]^{-T}([{}_rG_\phi^u]^{-1}\circ[{}_rH_{\phi\phi}^u])\cdot [{}_rG_\phi^u]^{-1} \tag{20}$$

The notation '$\circ$' in Eq. (20) denotes a generalized scalar dot product defined (refer to the Appendix).

The second-order kinematic relations between each minimum set and the output vector are given by

$$\ddot{\boldsymbol{\phi}}_b=[G_b^u]^{-1}\ddot{\boldsymbol{u}}+\dot{\boldsymbol{u}}^T[H_{uu}^b]\dot{\boldsymbol{u}} \tag{21}$$

$$\ddot{\boldsymbol{\phi}}_m=[G_m^u]^{-1}\ddot{\boldsymbol{u}}+\dot{\boldsymbol{u}}^T[H_{uu}^m]\dot{\boldsymbol{u}} \tag{22}$$

and

$$\ddot{\boldsymbol{\phi}}_t=[G_t^u]^{-1}\ddot{\boldsymbol{u}}+\dot{\boldsymbol{u}}^T[H_{uu}^t]\dot{\boldsymbol{u}} \tag{23}$$

where

$$[H_{uu}^b]=\begin{bmatrix}[{}_1H_{\phi\phi}^u]_{1;;}^{-1}\\ [{}_2H_{\phi\phi}^u]_{1;;}^{-1}\\ [{}_3H_{\phi\phi}^u]_{1;;}^{-1}\end{bmatrix} \tag{24}$$

$$[H_{uu}^m]=\begin{bmatrix}[{}_1H_{\phi\phi}^u]_{2;;}^{-1}\\ [{}_2H_{\phi\phi}^u]_{2;;}^{-1}\\ [{}_3H_{\phi\phi}^u]_{2;;}^{-1}\end{bmatrix} \tag{25}$$

and

$$[H_{uu}^t]=\begin{bmatrix}[{}_1H_{\phi\phi}^u]_{3;;}^{-1}\\ [{}_2H_{\phi\phi}^u]_{3;;}^{-1}\\ [{}_3H_{\phi\phi}^u]_{3;;}^{-1}\end{bmatrix} \tag{26}$$

The inverse relation of Eq. (21) is obtained as

$$\ddot{\boldsymbol{u}}=[G_a^u]\ddot{\boldsymbol{\phi}}_a+\dot{\boldsymbol{\phi}}_a{}^T[H_{aa}^u]\dot{\boldsymbol{\phi}}_a \tag{27}$$

where

$$[H_{aa}^u]=-([G_a^u]\circ([G_a^u]^T[H_{uu}^a][G_a^u])) \tag{28}$$

Substituting Eqs. (9) and (27) into Eqs. (22) and (23), and rearranging results in

$$\ddot{\boldsymbol{\phi}}_m=[G_a^m]\ddot{\boldsymbol{\phi}}_a+\dot{\boldsymbol{\phi}}_a{}^T[H_{aa}^m]\dot{\boldsymbol{\phi}}_a \tag{29}$$

$$\ddot{\boldsymbol{\phi}}_t=[G_a^t]\ddot{\boldsymbol{\phi}}_a+\dot{\boldsymbol{\phi}}_a{}^T[H_{aa}^t]\dot{\boldsymbol{\phi}}_a \tag{30}$$

where

$$[H_{aa}^m]=[G_a^u]^T[-([G_a^m]\circ[H_{uu}^a]) +[H_{uu}^m]][G_a^u] \tag{31}$$

$$[H_{aa}^t]=[G_a^u]^T[-([G_a^t]\circ[H_{uu}^a]) +[H_{uu}^t]][G_a^u] \tag{32}$$

Finally, combining Eqs. (29) and (30) results in the following relation:

$$\ddot{\boldsymbol{\phi}}_p=[G_a^p]\ddot{\boldsymbol{\phi}}_a+\dot{\boldsymbol{\phi}}_a^T[H_{aa}^p]\dot{\boldsymbol{\phi}}_a \tag{33}$$

where

$$[H_{aa}^p]=\begin{bmatrix}[H_{aa}^m]\\ [H_{aa}^t]\end{bmatrix} \tag{34}$$

2.2 Output compliance model

Let $\boldsymbol{\tau}=(\tau_1\ \tau_2\ \cdots\ \tau_n)^T$ and $\boldsymbol{f}=(f_1\ f_2\ \cdots\ f_m)^T$ be the input torque vector and the externally applied force vector, respectively. From Eq. (9), the differential relation between the output vector and the input vector can be expressed as

$$\boldsymbol{\delta u}=[G_a^u]\ \boldsymbol{\delta\phi}_a \tag{35}$$

Since the following relation holds from the virtual work principle,

$$\boldsymbol{d\phi}_a^T\boldsymbol{\tau}=\boldsymbol{du}^T\boldsymbol{f} \tag{36}$$

substituting Eq. (36) into Eq. (35) results in

$$\boldsymbol{\tau}=[G_a^u]^T\boldsymbol{f} \tag{37}$$

Provided that $[C_{\phi\phi}]$ and $[C_{uu}]$ represent the compliance matrices for the input vector and the output vector, respectively, the following relations hold:

$$\boldsymbol{\delta\phi}_a=[C_{\phi\phi}]\boldsymbol{\tau} \tag{38}$$

$$\boldsymbol{\delta u}=[C_{uu}]\boldsymbol{f} \tag{39}$$

The compliance matrix for the input vector $\boldsymbol{\phi}_a=({}_1\phi_1\ {}_2\phi_1\ {}_3\phi_1)^T$ is given by

$$[C_{\phi\phi}]=\begin{bmatrix}C_{1\phi1} & 0 & 0\\ 0 & C_{2\phi1} & 0\\ 0 & 0 & C_{3\phi1}\end{bmatrix} \tag{40}$$

Substituting Eqs. (37) and (38) into Eq. (35) results in the following relation

$$\begin{aligned}\boldsymbol{\delta u}&=[G_a^u]\boldsymbol{\delta\phi}_a\\ &=[G_a^u][C_{\phi\phi}]\boldsymbol{\tau}\\ &=[G_a^u][C_{\phi\phi}][G_a^u]^T\boldsymbol{f}\\ &=[C_{uu}]\boldsymbol{f}\end{aligned} \tag{41}$$

where the output compliance matrix is defined by

$$[C_{uu}]=[G_a^u][C_{\phi\phi}][G_a^u]^T \tag{42}$$

Due to the inverse relation between the stiffness matrix and the compliance matrix, the stiffness matrix in the output space is expressed as below:

$$[K_{uu}]=([G_a^u][K_{\phi\phi}]^{-1}[G_a^u]^T)^{-1} \tag{43}$$

where

$$[K_{uu}]=[C_{uu}]^{-1} \tag{44}$$

$$[K_{\phi\phi}]=[C_{\phi\phi}]^{-1} \tag{45}$$

The compliance matrix should be diagonal at an RCC point, which allows a completely decoupled operation among the three output directions of the given parallel mechanism. For the compliance matrix of Eq. (42) to be diagonal, the off-diagonal terms of (42) should be zero. The following Eq. (46) represents this condition (Kim, et. al., 1996):

$$\begin{bmatrix}C_{xy}\\ C_{x\phi}\\ C_{y\phi}\end{bmatrix}=[A]\begin{bmatrix}C_{\phi_1}\\ C_{\phi_2}\\ C_{\phi_3}\end{bmatrix}=\begin{bmatrix}0\\0\\0\end{bmatrix} \tag{46}$$

where

$$[A]=\begin{bmatrix}A_{11} & A_{12} & A_{13}\\ A_{21} & A_{22} & A_{23}\\ A_{31} & A_{32} & A_{33}\end{bmatrix} \tag{47}$$

Since the magnitude of each joint compliance is not zero, the above relation holds only when the determinant of A is zero. The sufficient conditions to satisfy this has been investigated (Kim, et. al., 1996a and 1996b). As the first condition, the mechanism should maintain symmetric configurations. As the second condition, three joint compliances should be attached at the same location of each chain (i. e, the base location of each chain) and they must have the same magnitude. In other words, when the mechanism satisfied the following relations

$$\begin{aligned}&{}_1l_n={}_2l_n={}_3l_n=l_n,\ \text{for } n=1,\ 2,\ 3\\ &{}_2\phi_1={}_1\phi_1+\frac{2}{3}\pi,\ {}_3\phi_1={}_1\phi_1+\frac{4}{3}\pi\\ &{}_1\phi_2={}_2\phi_2={}_3\phi_2,\ {}_1\phi_3={}_2\phi_3={}_3\phi_3\\ &C_{\phi_b}=C_{1\phi1}=C_{2\phi1}=C_{3\phi1}\end{aligned} \tag{48}$$

the mechanism has an RCC point at the middle of the moving ternary, at which the compliance matrix is completely diagonal and has the following characteristics:

$$C_{xxb}=C_{yyb}=\frac{2l_1^2(S_2^1)^2}{3}C_{\phi_b} \tag{49}$$

$$C_{\phi\phi b}=\frac{l_1^2(S_2^1)^2}{3l_3^2(S_3^1)^2}C_{\phi_b} \tag{50}$$

where C_{xxb} and C_{yyt} denote the translational compliances in the directions of x and y, $C_{\phi\phi b}$ denotes the rotational compliance about the z axis, and S_n^r and C_n^r represent $\sin({}_r\phi_n)$ and $\cos({}_r\phi_n)$, respectively. As shown in Eq. (49), the compliances in the translational directions are the same, and the translational component and the rotational component has the following relationship

$$\frac{C_{xxb}}{C_{\phi\phi b}}=\frac{l_3^2(S_3^1)^2}{2} \tag{51}$$

Also, similar relations hold for the second- and third minimum sets. Eqs. (52)-(54) and Eqs. (55)-(57) belong to the second and third minimum sets, respectively.

$$C_{xxm}=C_{yym}=\frac{2l_1^2l_2^2(S_2^1)^2}{3(l_1^2+l_2^2+2l_1l_2C_2^1)}C_{\phi m} \tag{52}$$

$$C_{\phi\phi m}=\frac{l_1^2l_2^2(S_2^1)^2}{3(l_2l_3S_3^1+l_1l_3S_{23}^1)^2}C_{\phi m} \tag{53}$$

$$\frac{C_{xxm}}{C_{\phi\phi m}}=\frac{2(l_2l_3S_3^1+l_1l_3S_{23}^1)^2}{(l_1^2+l_2^2+2l_1l_2C_2^1)} \tag{54}$$

$$C_{xxt}=C_{yyt}=\frac{2}{3}l_2^2(S_2^1)^2C_{\phi t} \tag{55}$$

$$C_{\phi\phi t}=\frac{l_2^2(S_2^1)^2}{3(l_2S_2^1+l_3S_{23}^1)^2}C_{\phi t} \tag{56}$$

and

$$\frac{C_{xxt}}{C_{\phi\phi t}}=2(l_2S_2^1+l_3S_{23}^1)^2 \tag{57}$$

It is observed from Eqs. (51), (54), and (57) that the compliance relations for the three different minimum sets are independent. This feature enables the system to create diverse compliance characteristics.

2.3 Compliance model for the system with redundant joint compliances

Here, we are interested in the independent control of the translational and rotational compliance components by utilizing redundant compliances. The stiffness matrices for the first, second, and third minimum sets ($\boldsymbol{\phi}_b$, $\boldsymbol{\phi}_m$, $\boldsymbol{\phi}_t$) are given as

$$[K_{ii}]=\begin{bmatrix} k_{1\phi i} & 0 & 0 \\ 0 & k_{2\phi i} & 0 \\ 0 & 0 & k_{3\phi i}\end{bmatrix},\ i=b,\ m,\ t \tag{58}$$

Provided that only small displacements are imposed on the system, the potential energy stored in the system is given by

$$\begin{aligned} P.E.&=\frac{1}{2}\sum_{i=b}^{t}\{\boldsymbol{d\phi}_i^T[K_{ii}]\boldsymbol{d\phi}_i\} \\ &=\frac{1}{2}\boldsymbol{du}^T\sum_{i=b}^{t}\{[G_u^i]^T[K_{ii}][G_u^i]\}\boldsymbol{du} \\ &=\frac{1}{2}\boldsymbol{du}^T[K_{uu}]\boldsymbol{du}\end{aligned} \tag{59}$$

where the stiffness matrix at the output location is defined by

$$[K_{uu}]=\sum_{i=b}^{t}\{[G_u^i]^T[K_{ii}][G_u^i]\} \tag{60}$$

Assuming that the compliance matrix for each minimum set is diagonal and that the equivalent diagonal elements of the three compliance matrices have the same magnitude, then Eq. (60) can be represented as

$$[K_{uu}]=\sum_{i=b}^{t}\{k_i[G_u^i]^T[G_u^i]\} \tag{61}$$

where

$$[K_{uu}]_{m;n}=\sum_{i=b}^{t}k_i\sum_{k=1}^{3}[G_u^i]_{k,m}[G_u^i]_{k,n} \qquad m,\ n=1,\ 2,\ 3 \tag{62}$$

In particular, when the system maintains any symmetric configuration, the magnitude of the nondiagonal elements of $[K_{uu}]$ are all zero, and the magnitudes of the two translational compliance elements are identical ($k_{xx}=k_{yy}$). Using the inverse relationship between the stiffness element and compliance element, the output stiffness matrix can be related to the joint compliance matrix as follows:

$$\boldsymbol{K}_u=[B]\boldsymbol{K}_\phi \tag{63}$$

where

$$\boldsymbol{K}_u=[1/C_{xx}\ \ 1/C_{\phi\phi}]^T \tag{64}$$

$$\boldsymbol{K}_\phi=[1/C_{\phi_b}\ \ 1/C_{\phi_m}\ \ 1/C_{\phi_t}]^T \tag{65}$$

and

$$[B]=\begin{bmatrix} C_{\phi_b}/C_{xxb} & C_{\phi m}/C_{xxm} & C_{\phi t}/C_{xxt} \\ C_{\phi_b}/C_{\phi\phi b} & C_{\phi m}/C_{\phi\phi m} & C_{\phi t}/C_{\phi\phi t}\end{bmatrix} \tag{66}$$

The general solution of Eq. (63) is described by

$$\boldsymbol{K}_\phi=[B]^+\boldsymbol{K}_u+([I]-[B]^+[B])\boldsymbol{\varepsilon} \tag{67}$$

where $[B]^+$ represents the Moore-Penrose pseudo-inverse solution of $[B]$. The first term on the right-hand side of Eq. (67) denotes a minimum norm solution, and the second term denotes a null-space solution, which does not influence the output stiffness, but can be utilized for developing additional secondary criteria.

In fact, stiffness modulation of K_u is possible just by considering any two sets out of the three minimum sets, in which case the dimension of matrix $[B]$ is 2×2.

2.4 Simulation

Assuming that joint compliances are attached redundantly to all of the system joints, compliance characteristics at RCC points are analyzed through simulation.

Assume that the base joint of a planar mechanism forms an equilateral triangle with lateral length $l_4=\sqrt{3}$. Also consider a symmetric configuration at which the rotation angle (ϕ) about the z-axis is 0°. When the magnitudes of every joint compliances are given to be 1, and l_1 is equal to 1, Fig. 2(a) ~ (c) represent the contours for out-

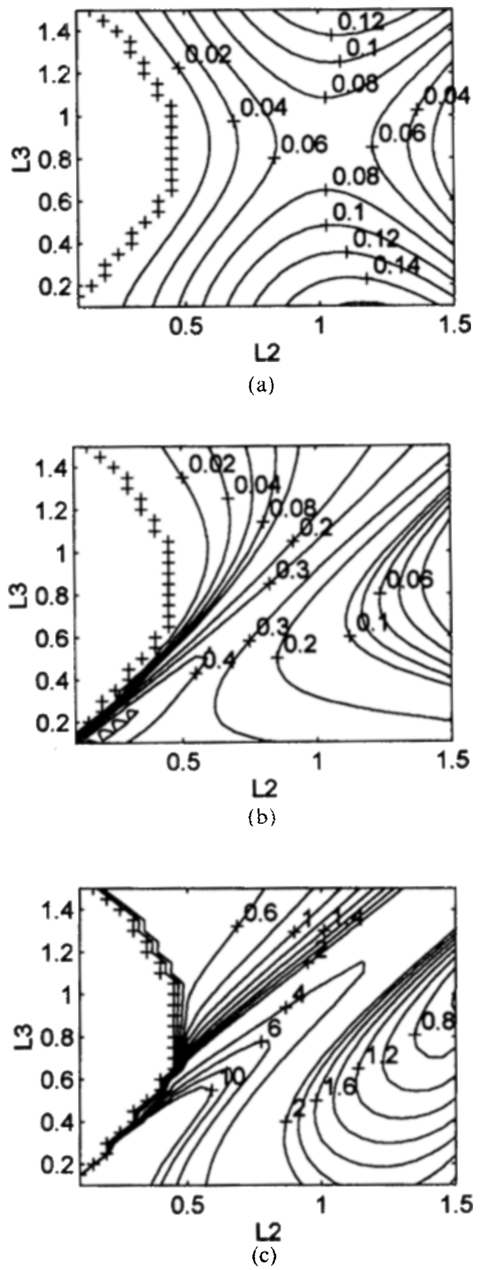

Fig. 2 Output compliances wrt. C_{ϕ_b}, C_{ϕ_m}, C_{ϕ_t}
(a) C_{xx} (b) $C_{\phi\phi}$ (c) $C_{\phi\phi}/C_{xx}$

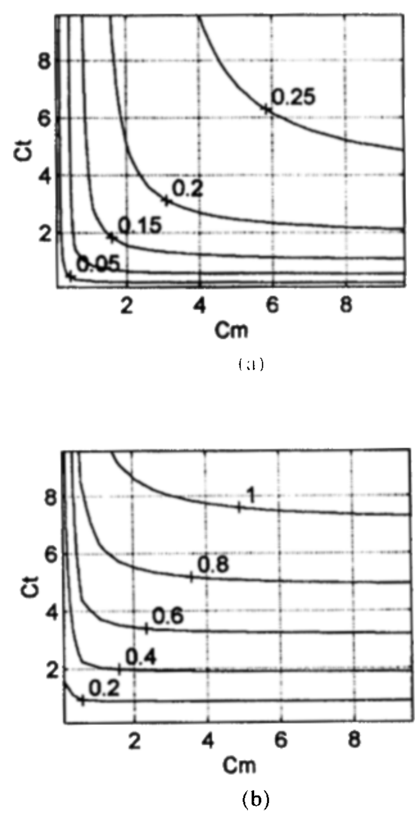

Fig. 3 Output compiances wrt, C_{ϕ_m}/C_{ϕ_b} vs. C_{ϕ_t}/C_{ϕ_b}
(for $C_{\phi_b}=1$, $l_1=0.9$, $l_2=0.8$, $l_3=0.3$)
(a) C_{xx} (b) $C_{\phi\phi}$

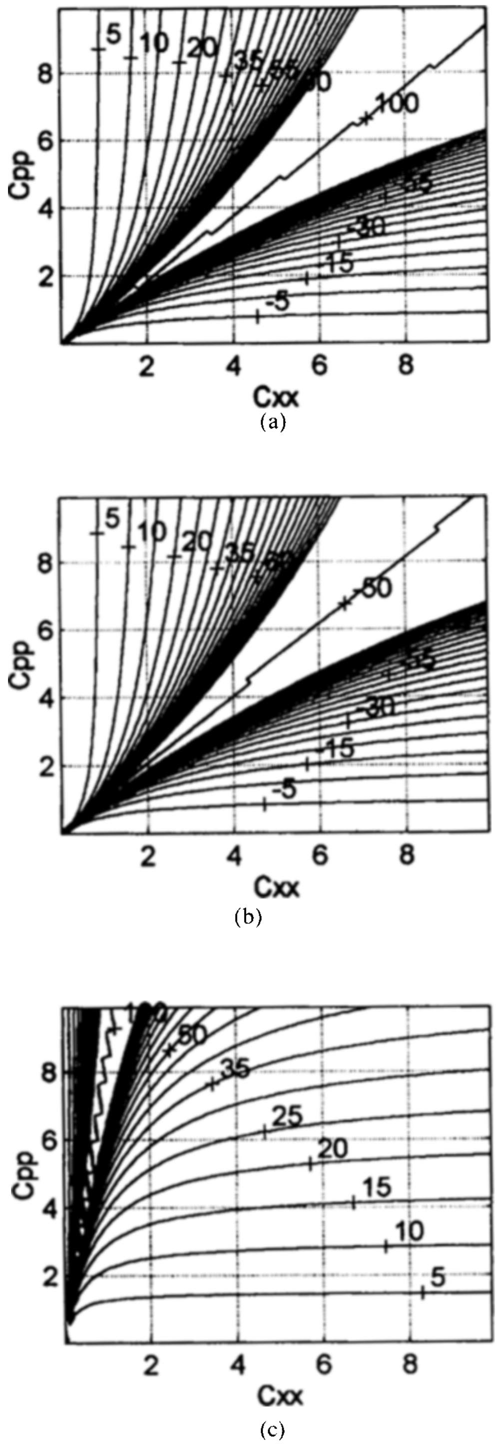

Fig. 4 Joint compliances wrt. C_{xx} vs. $C_{\phi\phi}$
(a) C_{ϕ_b} (b) C_{ϕ_m} (c) C_{ϕ_t}

put compliances with respect to the link lengths l_2 and l_3.

Also, consider a symmetric configuration with $\psi=0°$ and $C_{\phi_b}=1$. When the magnitudes of link length l_1, l_2, and l_3 are given as 0.9, 0.8, and 0.3, respectively, Fig. 3(a) ~ (c) represent the contours for translational and rotational output compliance elements with respect to the joint compliances C_{ϕ_m} and C_{ϕ_t}. It is observed from Figs. 2 and 3 that the output compliances are functions of link lengths and joint compliances.

For a symmetric configuration with $\psi=0°$ and the same link lengths as in the case of Fig. 3, Fig. 4(a) ~ (c) represent the contours for the joint compliances C_{ϕ_b}, C_{ϕ_m}, and C_{ϕ_t} (i. e., the first norm solution of Eq. (67)) with respect to the given translational and rotational output compliance elements.

If the solution of Eq. (67) yields negative joint compliances, we neglect this region and only consider those regions in which all three joint compliances are positive, since negative compliance cannot be realized by physical springs. It is observed that the output compliance matrix is always positive-definite for a positive-definite joint compliance matrix, but the joint compliance matrix is not always positive-definite for a desired positive-definite joint compliance matrix. Cutkosky and Kao also examined this fact in the stiffness analysis of multi-fingered hands (Cutkosky, et. al., 1989).

3. Compliance Modulation by Redundant Actuation

3.1 Analysis of stiffness created by antagonistic actuation

T_a and T_p represent the joint torque vectors for the independent joints and dependent joints, respectively. They are given by

$$T_a=(T_{a1}\ T_{a2}\ \cdots\ T_{aN})^T \tag{68}$$

$$T_p=(T_{p1}\ T_{p2}\ \cdots\ T_{pN})^T \tag{69}$$

The equilibrium equation expressed with respect to the minimum input coordinates is described by

$$T_a^* = T_a + [G_a^p]^T T_p = 0 \tag{70}$$

where T_a^* denotes an effective load vector at the minimum input coordinates. A linearized form of Eq. (70) with respect to the equilibrium position is

$$\frac{\partial T_a^*}{\partial \boldsymbol{\phi}_a} d\boldsymbol{\phi}_a = \frac{\partial T_a}{\partial \boldsymbol{\phi}_a} d\boldsymbol{\phi}_a + \frac{\partial}{\partial \boldsymbol{\phi}_a}([G_a^p]^T \boldsymbol{T}_p)\, d\boldsymbol{\phi}_a \tag{71}$$

where if $[K_{aa}]$ and $[K_{pp}]$ are defined as the stiffness matrices at the independent and dependent coordinates, respectively, and $[K_{aa}^e]$ as an effective stiffness matrix in the independent coordinates, then

$$[K_{aa}] = -\frac{\partial T_a}{\partial \boldsymbol{\phi}_a} \tag{72}$$

$$[K_{pp}] = -\frac{\partial T_p}{\partial \boldsymbol{\phi}_p} \tag{73}$$

and

$$[K_{aa}^e] = -\frac{\partial T_a^*}{\partial \boldsymbol{\phi}_a{}^*} \tag{74}$$

The second term of the right hand-side of Eq. (71) is given by

$$\frac{\partial}{\partial \boldsymbol{\phi}_a}([G_a^p]^T \boldsymbol{T}_p) = \boldsymbol{T}_p^T \circ [H_{aa}^p]^T - [G_a^p]^T [K_{pp}][G_a^p] \tag{75}$$

The stiffness matrix corresponding to the first -term of the right-hand side of Eq. (75) is given as follows:

$$\begin{bmatrix} \frac{\partial}{\partial \boldsymbol{\phi}_a}\left(\sum_{k=1}^{N_p} \frac{\partial \phi_{pk}}{\partial \phi_{a1}} (\boldsymbol{T}_p)_k\right) \\ \frac{\partial}{\partial \boldsymbol{\phi}_a}\left(\sum_{k=1}^{N_p} \frac{\partial \phi_{pk}}{\partial \phi_{ai}} (\boldsymbol{T}_p)_k\right) \\ \frac{\partial}{\partial \boldsymbol{\phi}_a}\left(\sum_{k=1}^{N_p} \frac{\partial \phi_{pk}}{\partial \phi_{aN_a}} (\boldsymbol{T}_p)_k\right) \end{bmatrix} \tag{76}$$

where $(\boldsymbol{T}_p)_k$ denotes the k^{th} element of the vector $\boldsymbol{T}_p$. Noting that the (i, j) element of the k^{th} plane of the second-order influence coefficient matrix $[H_{aa}^p]$ is defined as (Freeman, et. al., 1988)

$$[H_{aa}^p]_{k;i;j} = \frac{\partial}{\partial \phi_{ai}}\left(\frac{\partial \phi_{pk}}{\partial \phi_{aj}}\right) \tag{77}$$

the (i, j) element of Eq. (76) can be expressed as $(\boldsymbol{T}_p^T) \circ ([H_{aa}^p])_{:ji}$. Finally, the effective stiffness matrix expressed in terms of the independent coordinates is obtained as

$$[K_{aa}^*] = [K_{aa}] - \boldsymbol{T}_p^T \circ [H_{aa}^p]^T + [G_a^p]^T [K_{pp}][G_a^p] \tag{78}$$

where the first and third terms represent the stiffness matrices due to joint compliances attached to the independent and dependent coordinates, respectively, and the second term denotes the stiffness matrix created by antagonistic preloading between the independent coordinates and the dependent coordinates.

It has been known (Yi, et. al., 1993) that the effective stiffness matrix in the output position is given in terms of $[K_{aa}^*]$

$$[K_{uu}^*] = [G_u^a]^T [K_{aa}^*][G_u^a] \tag{79}$$

where $[G_u^a]$ is equivalent to $[G_u^b]$ when the independent coordinates are given as the first minimum set.

3.2 Analysis of antagonistic stiffness at RCC point

In this section, the characteristics of the antagonistic stiffness created by antagonistic preloading are analyzed without consideration of the joint compliance (or stiffness). Substituting the second -term of Eq. (78) into Eq. (79) yields

$$[K_{uu}^*] = [G_u^a]^T (-\boldsymbol{T}_p^T \circ [H_{aa}^p]^T) [G_u^a] \tag{80}$$

Then, Eq. (80) is equivalently expressed as the following equation

$$[K_{uu}^*] = -\boldsymbol{T}_p^T \circ ([G_u^a]^T [H_{aa}^p][G_u^a]) \tag{81}$$

where $\boldsymbol{T}_p$ satisfies the static equilibrium (Eq. (70)).

$[K_{uu}^*]$ has 6 independent stiffness elements due to its symmetry. When $[K_{uu}^*]$ is given by

$$[K_{uu}^*] = \begin{bmatrix} k_{xx} & k_{xy} & k_{x\varphi} \\ k_{yx} & k_{yy} & k_{y\varphi} \\ k_{\varphi x} & k_{\varphi y} & k_{\varphi\varphi} \end{bmatrix} \tag{82}$$

the six off-diagonal elements of $[K_{uu}^*]$ should be all zero to satisfy the condition for RCC point. The (m, n) element of Eq. (81) can be expressed by

$$[K_{uu}^*]_{mn} = -[[G_u^a]^T [H_{aa}^p][G_u^a]]_{:mn} \{\boldsymbol{T}_p\} \tag{83}$$

Yi and Freeman (1993) derived necessary conditions for stiffness modulation by antagonistic preloading in general redundantly actuated systems (refer to Appendix 2). According to those conditions, a planar system with three kinematic closed-loop chains has only two independent loops, and since each loop has two nonholonomic constraint equations in the planar mechanism, the system has 4 independent nonholonomic constraint equations, which allows modulation of the same number of stiffness elements. Therefore, only four out of six stiffness elements can be controlled independently.

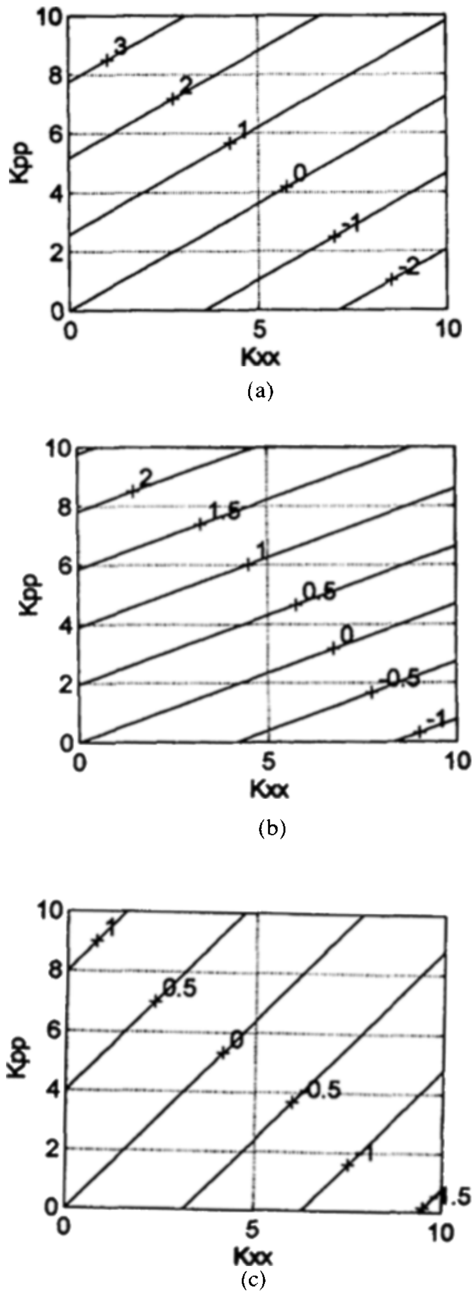

Fig. 5 Torque: (a) $T_b = T_a$ **(b)** T_m **(c)** T_t

While Yi and Freeman (1993) have considered general workspaces, here only a symmetric configuration is considered. It is numerically verified that in cases of symmetric configurations of the given planar mechanism, two out of three non-diagonal elements are independent and the other one has a dependent relation. Once two non-diagonal elements are zero, the other one becomes zero automatically. Also, in symmetric configurations, k_{xx} is always equivalent to k_{yy}. Therefore, we only need to control four stiffness elements $(k_{xy}, k_{x\psi}, k_{xx}, k_{\psi\psi})$. The relation between the four stiffness elements and the torque is expressed in the following matrix

$$\begin{bmatrix} k_{xx} \\ k_{\psi\psi} \\ k_{xy} \\ k_{x\psi} \end{bmatrix} = -\begin{bmatrix} ([G_u^a]^T[H_{aa}^p][G_u^a])_{;11} \\ ([G_u^a]^T[H_{aa}^p][G_u^a])_{;33} \\ ([G_u^a]^T[H_{aa}^p][G_u^a])_{;12} \\ ([G_u^a]^T[H_{aa}^p][G_u^a])_{;13} \end{bmatrix} \boldsymbol{T}_p \tag{84}$$

Equation (70) can be expressed in the following matrix form

$$[[I]_{3\times3}\ [G_a^p]^T]\,\boldsymbol{T}_\phi = \boldsymbol{0}_{3\times1} \tag{85}$$

where

$$\boldsymbol{T}_\phi = [\boldsymbol{T}_a^T\ \boldsymbol{T}_p^T]^T \tag{86}$$

Combining Eqs. (84) and (85) results in

$$\boldsymbol{y} = [D]\boldsymbol{T} \tag{87}$$

where

$$\boldsymbol{y} = [k_{xx}\ k_{\psi\psi}\ k_{xy}\ k_{x\psi}\ 0\ 0\ 0]^T \tag{88}$$

and the matrix $[D]$ with dimension 7×9 is given by

$$[D] = \begin{bmatrix} \boldsymbol{0}_{4\times3} & -\begin{bmatrix} ([G_u^a]^T[H_{aa}^p][G_u^a])_{;11} \\ ([G_u^a]^T[H_{aa}^p][G_u^a])_{;11} \\ ([G_u^a]^T[H_{aa}^p][G_u^a])_{;12} \\ ([G_u^a]^T[H_{aa}^p][G_u^a])_{;13} \end{bmatrix}_{4\times6} \\ [I]_{3\times3} & [G_a^p]^T{}_{3\times6} \end{bmatrix} \tag{89}$$

In Eq. (88), $k_{xy}=0$, $k_{x\psi}=0$, and k_{xx} and $k_{\psi\psi}$ are set to arbitrary values. Then, the solution of $\boldsymbol{T}$ from Eq. (87) is described by

$$\boldsymbol{T} = [D]^+\boldsymbol{y} + (I - D^+D)\,\boldsymbol{\varepsilon} \tag{90}$$

where $[D]^+$ denotes the Moore Penrose pseudo

-inverse of $[D]$, and the first term of Eq. (90) represents a minimum norm solution, and the second-term represents a null-space solution that can be utilized for stiffness modulation and other purposes. When all the link lengths of the mechanism are given as 0.5, and the magnitudes of k_{xy} and $k_{x\varphi}$ are set to zero, Fig. 5(a), 5(b), and 5(c) represent the contours for T_b, T_m, and T_t with respect to k_{xx} and $k_{\varphi\varphi}$ when only the minimum norm solution of Eq. (90) is considered.

4. Conclusions

Currently existing RCC devices are made of compliant passive structures, and thus they cannot adjust the magnitude of their compliances according to various task conditions (Whitney, 1986).

In this work, we investigate different types of RCC devices employing the structure of parallel mechanisms in order to obtain adjustable RCC characteristics. In our previous work, we verified that when three identical joint compliances are attached to the three base joints of the mechanism, an RCC point exists at the center of the ternary of the mechanism in its symmetric configurations, and that the magnitudes of two translational compliances are the same at an RCC point regardless of the magnitude of link lengths and joint compliances, and that the rotational compliance has some functional relation with the translational compliance. However, when employing a minimum number of (three) joint compliances, the translational and rotational compliances at the output (RCC) position cannot be independently controlled. Therefore, we suggest two methods for independent control of the translational and rotational compliances, by employing redundant joint compliances or redundant actuators. In the first approach, adaptable RCC characteristics are achieved purely by attaching different magnitudes of passive or decoupled feedback compliances to each minimum set. In the second approach, they are achieved by antagonistic redundant actuation among system actuators.

We conclude that redundancies of joint compliance or actuator play an important role in the modulation of the output compliance matrix. The completely decoupled compliance matrix at an RCC point is important for independent control of each direction at the given task position of robot manipulators. The basic theory of this paper will be applicable to the analysis of compliance characteristics of diverse parallel mechanisms.

Acknowledgement

This research is supported by the Korea Science and Engineering Foundation (No: 951-1008-079-2). The support of the KOSEF is greatly appreciated.

References

Brussel, H. V., Thielemans, H. and Simons, J., 1986, "Further Developments of the Active Adaptive Compliant Wrist (AACW) for Robot Assembly," *Proc. Int'l Symp. on Industrial Robots, SME*, pp. 377~384.

Cutkosky, M. R. and Kao, I., 1989, "Computing and Controlling the Compliance of a Robotic Hand," *IEEE Transaction. of Robotics and Automation*, Vol. 5, No. 2, pp. 151~165.

Freeman, R. A. and Tesar, D., 1988, "Dynamic Modeling of Serial and Parallel Mechanisms/Robotic Systems, Part I-Methodology, Part II-Applications," *Proceedings of 20th ASME Mechanisms Conference*, Orlando, FL.

Kang, H. J., Yi, B. J., Cho, W. and Freeman, R. A., 1990, "Constraint-embedding Approaches for General Closed-Chain System Dynamics in Terms of A Minimum Coordinate Set," *Proc. of 1990 ASME Mechanism/Design Conf.*, DE-Vol. 24, pp. 125~132.

Kim, W. K., Lee, J. Y. and Yi, B. J., 1996, "RCC Characteristics of Planar/Spherical 3-Degree-of- Freedom Parallel Mechanisms with Joint Compliances," *'96 IROS*, Osaka, Japan.

Kim, W. K., Lee, J. Y. and Yi, B. J., 1996, "Analysis of a Planar 3 Degree-of-Freedom Adjustable Compliance Mechanism," *KSME Journal*, Vol. 10, No. 3.

McCallion, H., Alexander, K. V. and Pham, D.

T., 1980, "Aid for Automatic Assembly," *1st Int'l Conf. on Assembly Automation*, pp. 313~323.

Peshkin, M. A., 1990, "Programmed Compliance for Error Corrective Assembly," *IEEE Trans. on Robotics and Automation*, Vol. 6, No. 4, pp. 474~482.

Whitney, D. E., 1986, "Remote Center Compliance," in *Encyclopedia of Robotics System and Control*," Vol. 2, pp. 1316~1324, edited by J. J. Diponio and Y. Hasegawa, published by Industrial Training Corporation.

Yi, B. J. and Freeman, R. A., 1993, "Geometric Analysis of Antagonistic Stiffness in Redundantly Actuated Parallel Mechanisms," *Journal of Robotic Systems*, Vol. 10, No. 5, pp. 581~603.

Appendix 1

Operator '$\circ$' is called the generalized dot product and is defined as follows: let A and B represent a $p\times q$ matrix and a three-dimensional $q\times(m\times n)$ array. The resulting $p\times(m\times n)$ array C is obtained as

$$C_{pij}=[A\circ B]_{pij}=\sum_{k=1}^{a}A_{pk}B_{kij}$$

Appendix 2

Necessary Condition for Full Stiffness Generation in Redundantly Actuated Parallel Mechanisms

A closed-chain mechanism is capable of full stiffness generation only if it satisfies

$$J_a\geq D+M$$

where

D: number of independent stiffness elements $(=M(M+1)/2)$

M: degrees of freedom (system mobility)

J_a: number of active joints

and

$$NC=(IC-LC)\geq D$$

where

IC: number of independent constraint equations

NC: number of dependent constraint equations

LC: number of independent linear constraint equations.